



## Sensitivity of Love surface waves to mass loading

P. Kielczyński

*Institute of Fundamental Technological Research, Polish Academy of Sciences, ul. Pawińskiego 5B, 02-106 Warsaw, Poland*

### ARTICLE INFO

#### Keywords:

Love wave waveguides  
Analytical modeling of Love wave devices  
Mass sensitivity  
Dispersion curves  
Optimization of Love wave sensors

### ABSTRACT

The sensitivity of the phase velocity  $v_p$  of Love surface waves to mass loading is a very important characteristic of Love wave devices. In this paper, we present a novel approach to evaluate the sensitivity of Love surface waves to loading with an infinitesimal layer of mass of a surface density  $\sigma$  [ $\text{kg}/\text{m}^2$ ]. To this end, we developed analytical formulas for the mass coefficient of sensitivity  $S_\sigma^v = (1/v_p)dv_p/d\sigma$  [ $\text{m}^2/\text{kg}$ ] and phase velocity gradients  $-dv_p(f)/df$  and  $-dv_p(h_1)/dh_1$ , where  $f$  and  $h_1$  stand, respectively, for frequency of the Love wave and thickness of the guiding surface layer. We also established analytical formulas that relate the mass sensitivity  $S_\sigma^v$  with 1) the relative slope (gradient)  $-(1/v_p)dv_p/dh_1$  of the phase velocity dispersion curve  $v_p(h_1)$ , and 2) the relative slope (gradient)  $-(1/v_p)dv_p/df$  of the phase velocity dispersion curve  $v_p(f)$ . These analytical formulas have been developed using full wave theory. We have discovered that the maxima of the mass sensitivity  $S_\sigma^v(f)$ ,  $S_\sigma^v(h_1)$  and maxima of the relative gradients  $-(1/v_p)dv_p/df$ ,  $-(1/v_p)dv_p/dh_1$ , occur virtually at the same values of  $f$  and  $h_1$ . Comparing with the Perturbation Method and Finite Element Method (FEM), the analytical formulas established in this paper display some advantages, such as very low execution time of the mass sensitivity, and perhaps more importantly a possibility for a direct parametric optimization of the Love wave waveguide as a function of its material parameters, thickness of the guiding surface layer and wave frequency.

### 1. Introduction

Due to high concentration of the Love wave energy in the guiding surface layer of the waveguide, Love wave devices can achieve very high sensitivities to surface loading with a thin layer of a lossless mass or an infinite layer of a lossy viscoelastic liquid [1–3]. Shear horizontal (SH) surface waves of the Love type have only one SH component of mechanical vibrations that is parallel to the free surface of the waveguide. Therefore, Love surface waves are naturally destined for use in devices operating in a liquid environment [4–13], since they are very little attenuated by liquids of a moderate viscosity. By contrast, Love surface waves can be considerably affected by loading with a thin layer of lossless mass (phase changes) or with an infinite layer of a lossy viscoelastic liquid (phase changes and amplitude attenuation).

An infinitesimally thin layer of lossless mass of a surface density  $\sigma$  [ $\text{kg}/\text{m}^2$ ], loading the waveguide, alters the phase velocity  $v_p$  of the Love wave, without introducing any extra attenuation of the Love wave.

The mass sensitivity  $S_\sigma^v = (1/v_p)(dv_p/d\sigma)$  quantifies changes in the phase velocity  $v_p$  of the Love wave caused by an infinitesimally thin layer of mass of surface density  $\sigma$  loading the waveguide. The mass sensitivity  $S_\sigma^v$ , although inherited from older types of ultrasonic devices

(quartz micro-balance, QCM), is one of the most important parameters characterizing the quality of Love wave devices.

In an optimum design process, including Love wave devices, it is prerequisite to develop an adequate mathematical model of the device that includes all its vital parameters.

The problem of determining the mass sensitivity of Love wave devices (sensors) was previously investigated in References [14–20], where the authors employed Perturbation Method and the Finite Element Method (FEM).

Perturbation Methods are valid, by definition, only for small changes in the physical parameters no higher than say a few %. For this reason, Perturbation Methods are always approximate and provide the solutions that are always different from closed-form analytical solutions of the analyzed problem.

Since the FEM method can include a large number of parameters, such as piezoelectricity, nonlinearity, etc. it is the most general and versatile method comparing with analytical and perturbation methods. The FEM method is a very powerful tool in analysis of real (practical) structures of Love wave devices with waveguides of complex geometry, displaying anisotropy and/or a piezoelectric effect. Moreover, the FEM method can cope with the second order effects such as: reflections from the waveguide surfaces, leaky and bulk wave propagation, etc.

E-mail address: [pkielczy@ippt.pan.pl](mailto:pkielczy@ippt.pan.pl).

<https://doi.org/10.1016/j.sna.2022.113465>

Received 25 April 2021; Received in revised form 28 January 2022; Accepted 22 February 2022

Available online 24 February 2022

0924-4247/© 2022 Elsevier B.V. All rights reserved.

However, these advantages are counterbalanced by a significant increase in the computing time. For example, complicated FEM 3D simulations can take days or weeks [19], depending on the number of available CPUs and RAM memory of the computer.

In the present paper we have adopted different approach that is devoid of simplifications inherent for the Perturbation Method. Namely, to determine the mass sensitivity of the Love wave device, we first solved the equations of motion in the subsequent layers of the waveguide. Then, after imposing the boundary conditions, we developed the dispersion equation for phase velocity of Love surface waves. Subsequently, using the rules of differentiation of implicit functions we obtained the equations for the mass sensitivity of Love surface waves in a closed analytical form that are valid for an arbitrarily high surface mass loading  $\sigma$ .

The analytical model presented in this paper was developed under the following simplifying assumptions:

- 1) Elastic materials of the surface layer and substrate are linear, isotropic, lossless and homogeneous in all directions.
- 2) Piezoelectric effect is neglected.
- 3) Elastic waveguide is semi-infinite in the transverse direction and infinite in the remaining two directions.
- 4) Generation and detection of Love surface waves is out of scope of this paper.
- 5) Spurious bulk and subsurface waves have been neglected.
- 6) Material constants of the waveguide are constant and do not change with temperature or frequency.

The execution time, with the developed Analytical Method and an equivalent Perturbation Method, is virtually the same, namely of the order of a fraction of a second. However, the Analytical Method developed in this paper provides us much deeper insight into the physical phenomena occurring in the Love wave waveguide.

In contrast to Perturbation Methods, valid only for small changes in parameters of the waveguide, the Analytical Method developed in this paper is valid for an arbitrarily high surface mass loading  $\sigma$  of Love wave waveguides.

In addition to the mass sensitivity  $S_{\sigma}^{v_p}$ , the author has developed analytical formulas for the phase velocity gradients  $-dv_p/df$  and  $-dv_p/dh_1$ , where  $f$  and  $h_1$  stand, respectively, for the frequency of the Love wave and thickness of the guiding surface layer. We have found that the maxima of the mass coefficient of sensitivity  $S_{\sigma}^{v_p}(f)$ ,  $S_{\sigma}^{v_p}(h_1)$  and maxima of the relative gradients  $-(1/v_p)dv_p/df$ ,  $-(1/v_p)dv_p/dh_1$ , occur virtually at the same point of  $f$  and  $h_1$  what was not yet published in the literature.

Another new result obtained by the author are analytical formulas (Eqs. 24 and 26) that relate the mass sensitivity  $S_{\sigma}^{v_p}$  of Love surface waves with both 1) the relative gradient  $-(1/v_p)dv_p/dh_1$  of the dispersion curve  $v_p(h_1)$  and 2) the relative gradient  $-(1/v_p)dv_p/df$  of the dispersion curve  $v_p(f)$ .

The use of the developed analytical formulas for the mass sensitivity  $S_{\sigma}^{v_p}$  (Eq.18) and the relative phase velocity gradients  $-(1/v_p)dv_p/df$ ,  $-(1/v_p)dv_p/dh_1$  (Eqs. 20 and 22) can be very useful in the design of Love wave devices giving us direct and quick insight in physical phenomena occurring in Love wave waveguides, such as dependence of the mass coefficient  $S_{\sigma}^{v_p}$  on material parameters of the Love wave waveguide, thickness of the guiding surface layer  $h_1$ , wave frequency  $f$ , etc.

Despite many simplifying assumptions, the Analytical Method, developed in this paper, can provide reasonably accurate results applicable in design and optimization of Love wave devices. Thus, it can be considered as a valuable complement for the more versatile and exact FEM method with many software packages that are available commercially.

## 2. Physical model

In this paper, we analyze properties of Love surface waves propagating in waveguides consisting of a guiding PMMA surface layer ( $0 < x_2 \leq h_1$ ) deposited on a semi-infinite ST-cut Quartz substrate ( $x_2 > h_1$ ). Losses in the PMMA surface layer are neglected. In addition, top surface of the guiding surface layer is covered with an infinitesimally thin layer of mass with a surface density  $\sigma$  [ $\text{kg}/\text{m}^2$ ], see Fig. 1.

Material and geometrical parameters of the analyzed Love wave waveguide structure are given in Table 1.

An important property of Love surface waves is their unique vibration pattern with one non-zero shear-horizontal (SH) component of vibrations (mechanical displacement  $u_3$ ), which is polarized along the  $x_3$  axis, parallel to the free surface ( $x_2 = 0$ ) of the waveguide and perpendicular to the direction of propagation of the Love wave along the  $x_1$  axis. The  $x_2$  axis points into the bulk of the substrate. All material parameters of the layered waveguide may change only along the  $x_2$  axis but are homogeneous and isotropic along the  $x_1$  and  $x_3$  axes.

Since Love surface waves analyzed in this paper propagate in the lossless waveguide structure shown in Fig. 1 the wave number  $k$  of the Love wave is a real-valued quantity and equals  $k = \omega/v_p$ , where  $\omega$  is the angular frequency of the Love wave and  $v_p$  its phase velocity.

Phase velocity of bulk SH waves in the PMMA (Poly(methyl methacrylate)) guiding surface layer equals  $v_1 = 1100$  m/s and in the ST-cut Quartz substrate  $v_2 = 5060$  m/s (see Table 1). Love surface waves can exist only in waveguides with slower guiding surface layer than the substrate ( $v_1 < v_2$ ). The waveguide analyzed in this paper was designed to fulfill this necessary condition. It is interesting to note that Quartz is the only common piezoelectric material that can support pure SH bulk waves [24] and therefore is often used as a substrate in Love wave waveguides.

## 3. Theoretical background (Direct Sturm-Liouville Problem)

The propagation of Love surface waves in the waveguide structure shown in Fig. 1 is governed by the wave equation [25,26] in the constituent regions of the waveguide in conjunction with the appropriate boundary conditions, [27], on the upper surface of the guiding surface layer  $x_2 = 0$  and at the interface  $x_2 = h_1$  between the surface layer and the substrate.

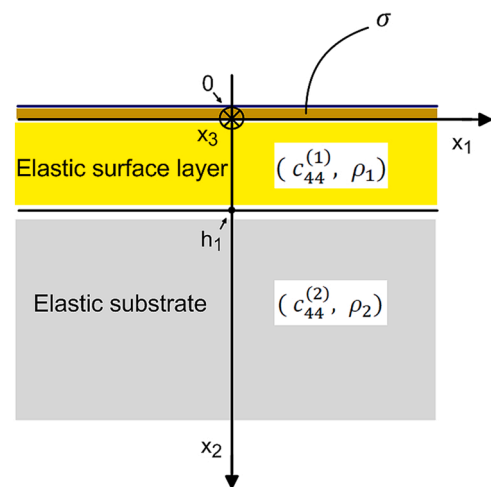


Fig. 1. Cross-section of the analyzed Love wave waveguide loaded with an infinitesimally thin layer of mass with a surface density  $\sigma$  [ $\text{kg}/\text{m}^2$ ]. Love surface waves propagate in the direction of axis  $x_1$ . Shear horizontal (SH) mechanical displacement  $u_3$  of the Love wave is polarized along the  $x_3$  axis.

**Table 1**  
Material and geometrical parameters of the analyzed Love wave waveguide [21–23].

Material	Thickness [μm]	Density [kg/m <sup>3</sup> ]	Storage shear modulus [GPa]	SH wave velocity [m/s]
PMMA surface layer	$h_1 = 0 - 8$	$\rho_1 = 1180$	$c_{44}^{(1)} = 1.43$	$v_1 = 1100$
ST-cut Quartz substrate	semi-infinite	$\rho_2 = 2650$	$c_{44}^{(2)} = 67.85$	$v_2 = 5060$

### 3.1. Governing differential equations

#### 3.1.1. Lossless elastic surface layer ( $0 < x_2 < h_1$ )

The mechanical displacement  $u_3^{(1)}$  of the Love wave in the elastic surface layer fulfills the following wave equation:

$$\frac{1}{v_1^2} \frac{\partial^2 u_3^{(1)}}{\partial t^2} = \frac{\partial^2 u_3^{(1)}}{\partial x_1^2} + \frac{\partial^2 u_3^{(1)}}{\partial x_2^2} \quad (1)$$

where:  $v_1 = (c_{44}^{(1)}/\rho_1)^{1/2}$  is the phase velocity of bulk SH waves in the elastic surface layer,  $c_{44}^{(1)}$  is its storage modulus and  $\rho_1$  is the density of the elastic surface layer.

#### 3.1.2. Semi-infinite elastic substrate ( $x_2 > h_1$ )

The mechanical displacement  $u_3^{(2)}$  of the Love wave in the elastic substrate satisfies the following partial differential equation (wave

$$\left[ \begin{array}{c} V \\ T \end{array} \right] \Big|_{x=h_1} = \cos(q_1 \bullet h_1) * \left[ \begin{array}{cc} 1 & \frac{1}{c_{44}^{(1)} \bullet q_1} \tan(q_1 \bullet h_1) \\ -c_{44}^{(1)} \bullet q_1 \bullet \tan(q_1 \bullet h_1) & 1 \end{array} \right] * \left[ \begin{array}{c} V \\ T \end{array} \right] \Big|_{x=0} = \begin{bmatrix} A_{11} & A_{12} \\ A_{21} & A_{22} \end{bmatrix} * \left[ \begin{array}{c} V \\ T \end{array} \right] \Big|_{x=0} \quad (6)$$

equation):

$$\frac{1}{v_2^2} \frac{\partial^2 u_3^{(2)}}{\partial t^2} = \frac{\partial^2 u_3^{(2)}}{\partial x_1^2} + \frac{\partial^2 u_3^{(2)}}{\partial x_2^2} \quad (2)$$

where:  $v_2 = (c_{44}^{(2)}/\rho_2)^{1/2}$  is the phase velocity of the bulk SH waves in the elastic substrate,  $c_{44}^{(2)}$  its storage modulus of elasticity and  $\rho_2$  is the density of the elastic substrate.

### 3.2. Derivation of the dispersion relation for Love surface waves using Transfer Matrix Method

The dispersion equation of Love surface waves propagating in the layered waveguide presented in Fig. 1 has been derived in this paper using the Transfer Matrix Method (TMM) developed previously by Thomson and Haskell in seismology [28–30].

The key property of the TMM method is the relation between the mechanical displacement  $u_3$  and shear stress  $\tau_{23}$  of the Love wave on the upper surface of the surface layer with the mechanical displacement and shear stress on the lower surface of the layer. Below we will sketch briefly the derivation of this relationship.

A general form of the time-harmonic mechanical displacement  $u_3(x_1, x_2, t)$  of the Love surface wave, propagating in the direction  $x_1$ , and uniform along the axis  $x_3$ , will be sought in the following form:

$$u_3(x_1, x_2, t) = V(x_2) \bullet \exp[j(kx_1 - \omega t)] \quad (3)$$

where:  $V(x_2)$  is the mechanical displacement  $u_3(x_2)$  of the Love wave, as

a function of depth  $x_2$ ,  $k$  is the wave number of the Love wave and  $\omega$  its angular frequency.

The shear stress  $\tau_{23}(x_1, x_2, t)$  associated with the mechanical displacement  $u_3(x_1, x_2, t)$  of the Love wave is given by the following formula:

$$\tau_{23}(x_1, x_2, t) = T(x_2) \bullet \exp[j(kx_1 - \omega t)] \quad (4)$$

where:  $T(x_2) = c_{44}(x_2) \partial V(x_2) / \partial x_2$  and  $c_{44}(x_2)$  is the shear modulus of elasticity in the constituent parts of the waveguide, namely, guiding surface layer  $0 < x_2 < h_1$  and substrate  $h_1 < x_2$ .

Substituting Eq.3 into Eqs. 1 and 2 one obtains two ordinary differential equations of the second order. Introducing subsequently two new dependent variables: ( $V$  and  $T$ ), each second order differential equation, resulting from Eqs. 1 and 2, can be represented as a system of two differential equations of the first order, as follows:

$$\frac{d}{dx} \begin{bmatrix} V \\ T \end{bmatrix} = \begin{bmatrix} 0 & \frac{1}{c_{44}(x)} \\ \beta^2 c_{44}(x) - \omega^2 \rho(x) & 0 \end{bmatrix} \begin{bmatrix} V \\ T \end{bmatrix} \quad (5)$$

It can be shown that Eq.5 represents the Direct-Sturm-Liouville Problem for the eigenvalues  $\beta^2$  and the eigenvectors  $V$ .

Solving matrix differential Eq.5 for the PMMA guiding surface layer, we arrive at the following formula (Eq.6) that links the mechanical displacement and shear stress on the upper surface of the PMMA surface layer for ( $x_2 = 0$ ) with the mechanical displacement and shear stress on the lower surface of this layer ( $x_2 = h_1$ ), i.e.,

where:  $q_1 = \sqrt{k_1^2 - k^2}$  is the transverse wavenumber of the Love wave in the PMMA surface layer,  $k_1 = \omega/v_1$ ,  $v_1$  is the phase velocity of bulk SH waves in the PMMA surface layer,  $k$  is the real wave number of the Love wave and  $[A]$  is the transfer matrix defined by Eq.6. More details about the derivation of Eq.6 can be found in [8].

The transfer matrix  $[A]$  derived in Eq.6 can be written explicitly as:

$$[A] = \begin{bmatrix} A_{11} & A_{12} \\ A_{21} & A_{22} \end{bmatrix} = \begin{bmatrix} \cos(q_1 \bullet h_1) & \frac{1}{c_{44}^{(1)} \bullet q_1} \sin(q_1 \bullet h_1) \\ -c_{44}^{(1)} \bullet q_1 \bullet \sin(q_1 \bullet h_1) & \cos(q_1 \bullet h_1) \end{bmatrix} \quad (7)$$

The unknown components of the mechanical displacement and the corresponding shear stress, of the Love wave at the interface  $x_2 = 0$  and  $x_2 = h_1$  will be further denoted by  $V_0, T_0$  and  $V_D, T_D$ , respectively. Consequently, Eq.6 can written as

$$\begin{bmatrix} V_D \\ T_D \end{bmatrix} = \begin{bmatrix} A_{11} & A_{12} \\ A_{21} & A_{22} \end{bmatrix} \begin{bmatrix} V_0 \\ T_0 \end{bmatrix} \quad (8)$$

#### 3.3. Shear stresses on top $T_0$ and bottom $T_D$ of the PMMA guiding surface layer

Top surface of the PMMA surface layer ( $x_2 = 0$ ) is loaded with an infinitesimally thin layer of mass, with a surface density  $\sigma$ .

It can be shown that the shear stress  $T_0$  of the SH Love wave at the interface  $x_2 = 0$  with the infinitesimal layer of mass, of a surface density  $\sigma$ , can be expressed as

$$T_0 = -\sigma \bullet \omega^2 V_0 \tag{9}$$

This dependence emphasizes the inertial character of the loading with an infinitesimally thin layer of mass with a surface density  $\sigma$ .

The bottom of the guiding surface layer (PMMA) ( $x_2 = h_1$ ) is rigidly bonded to the semi-infinite elastic substrate (Quartz). The mechanical displacement  $V(x_2)$  of the Love wave in the elastic substrate is given by:  $V(x_2) = V_D \bullet \exp(-b \bullet x_2)$ . Consequently, the shear stress in the elastic substrate at the interface  $x_2 = h_1$  with the guiding surface layer (PMMA) is given by:

$$T_D = c_{44}^{(2)} \frac{\partial V}{\partial x_2} \Big|_{(x_2=h_1)} = -c_{44}^{(2)} \bullet b \bullet V_D \tag{10}$$

where:  $b = (k^2 - k_2^2)^{1/2}$ ;  $k_2 = \omega/v_2$  and  $v_2 = (c_{44}^{(2)}/\rho_2)^{1/2}$ . The variables  $b$  and  $k_2$  correspond, respectively, to the transverse wavenumber of the Love surface wave in the substrate and the wavenumber of bulk SH waves therein.

Substituting Eqs. 9 and 10 into Eq. 8 one obtains:

$$\left[ \begin{array}{c} V_D \\ -c_{44}^{(2)} \bullet b \bullet V_D \end{array} \right] \Big|_{x=h_1} = \left[ \begin{array}{cc} A_{11} & A_{12} \\ A_{21} & A_{22} \end{array} \right] \bullet \left[ \begin{array}{c} V_0 \\ -\sigma \bullet \omega^2 \bullet V_0 \end{array} \right] \Big|_{x=0} \tag{11}$$

Closer examination of Eq. 11 reveals that it contains only two unknown quantities, namely,  $V_0$  and  $V_D$ . By a simple rearrangement of terms in Eq. 11 we finally get a system of two linear homogeneous algebraic equations for  $V_0$  and  $V_D$ , in the following form:

$$\left[ \begin{array}{cc} 1, & -(A_{11} - A_{12} \bullet \sigma \bullet \omega^2) \\ c_{44}^{(2)} \bullet b, & (A_{21} - A_{22} \bullet \sigma \bullet \omega^2) \end{array} \right] \bullet \left[ \begin{array}{c} V_D \\ V_0 \end{array} \right] = \left[ \begin{array}{c} 0 \\ 0 \end{array} \right] \tag{12}$$

#### 4. Dispersion equation

A set of two linear algebraic equations for  $V_0$  and  $V_D$  has a non-trivial solution if the determinant of the left-hand-side matrix in Eq.12 vanishes. This condition leads to the following dispersion equation for Love waves, propagating in the investigated waveguide structure, shown in Fig. 1:

$$(A_{21} - A_{22} \bullet \sigma \bullet \omega^2) + (c_{44}^{(2)} \bullet b) \bullet (A_{11} - A_{12} \bullet \sigma \bullet \omega^2) = 0 \tag{13}$$

Substituting elements of the matrix [A] from Eq.7 into Eq.13, we arrive at the following dispersion equation for the Love surface waves propagating in the analyzed lossless waveguide structure, depicted in Fig. 1:

$$\tan(q_1 \bullet h_1) \bullet \left\{ (c_{44}^{(1)} \bullet q_1)^2 + (\sigma \bullet \omega^2) \bullet (c_{44}^{(2)} \bullet b) \right\} + (c_{44}^{(1)} \bullet q_1) \bullet \left\{ (\sigma \bullet \omega^2) - (c_{44}^{(2)} \bullet b) \right\} = F(v_p, \sigma, h_1, f) = 0 \tag{14}$$

where:  $k_1 = \omega/v_1$ ;  $k_2 = \omega/v_2$ ;  $q_1 = \sqrt{k_1^2 - k^2}$ ;  $b = \sqrt{k^2 - k_2^2}$ ;  $\sigma$  is the

$$S_\sigma^{v_p} = \frac{\omega^2 \frac{1}{k} \left\{ (c_{44}^{(1)} q_1) + (c_{44}^{(2)} b) \bullet \tan(q_1 h_1) \right\}}{\frac{h_1}{\cos^2(q_1 h_1)} \frac{\partial q_1}{\partial k} \left\{ (c_{44}^{(1)} q_1)^2 + (c_{44}^{(2)} b) (\sigma \omega^2) \right\} + \tan(q_1 h_1) \left\{ 2q_1 (c_{44}^{(1)})^2 \frac{\partial q_1}{\partial k} + c_{44}^{(2)} \frac{\partial b}{\partial k} (\sigma \omega^2) \right\} + c_{44}^{(1)} \frac{\partial q_1}{\partial k} \bullet \left\{ (\sigma \omega^2) - (c_{44}^{(2)} b) \right\} - c_{44}^{(2)} \frac{\partial b}{\partial k} (c_{44}^{(1)} q_1)} \tag{18}$$

surface mass density loading the surface of the waveguide,  $k$  is the real wavenumber of the Love wave and  $v_p = \omega/k$  is the phase velocity of the Love wave at an angular frequency  $\omega$ .

The dispersion equation Eq.14 is of primary importance in analysis of Love surface waves, since it enables the determination of the phase

velocity  $v_p$  of the Love wave, as a function of frequency  $f$  and the thickness  $h_1$  of the guiding surface layer. In fact, the determination of the dispersion equation is the necessary first step in analysis of Love surface waves, propagating in any surface waveguide.

Equation No 14 is an implicit relation between the phase velocity  $v_p$  of the Love wave propagating in the waveguide with material and geometrical parameters of the waveguide, shown in Fig. 1.

The dispersion equation (Eq.14) can be written in a more abstract form as:

$$F(c_{44}^{(1)}, \rho_1, c_{44}^{(2)}, \rho_2, \sigma, h_1, \omega; k) = 0 \tag{15}$$

Eq. 15 has the form of a nonlinear transcendental algebraic equation with only one unknown, i.e., the wavenumber  $k = \omega/v_p$  of the Love surface wave. The parameters in Eq. 15 are the following:  $c_{44}^{(1)}, \rho_1, c_{44}^{(2)}, \rho_2, \sigma, h_1$  and  $\omega$ . It is rather not realistic to expect that any closed form solution for the algebraic Eq. 15 would emerge, regardless how hard we might work. Therefore, the nonlinear algebraic Eq. 15 has to be solved numerically.

The nonlinear algebraic Eq. 15 was solved in this paper numerically using specialized procedures provided by the computer package Scilab. Since the analyzed waveguide is lossless the wave number  $k$  of the Love wave determined from Eq.15 must be a real-valued quantity.

#### 5. Mass sensitivity $S_\sigma^{v_p}$ of Love surface waves

The sensitivity of Love surface waves to loading with an infinitesimal layer of mass, of a surface density  $\sigma$ , can be quantified by the following coefficient of mass sensitivity  $S_\sigma^{v_p}$  defined as [1]:

$$S_\sigma^{v_p} = \frac{1}{v_p} \left( \frac{dv_p}{d\sigma} \right) \tag{16}$$

Since in lossless waveguide structures, such as those analyzed in this paper (see Fig. 1), the phase velocity  $v_p = \omega/k$  of the Love wave is always a real-valued quantity. Consequently, by virtue of Eq.16, the same can be said about the mass coefficient of sensitivity  $S_\sigma^{v_p}$ .

The dispersion Eq. (14) is an implicit function of the phase velocity  $v_p$  and surface mass density  $\sigma$ , what can be symbolically written as  $F(v_p, \sigma) = 0$  (see also Eq.15). The derivative  $dv_p/d\sigma$  in Eq. 16 can be calculated analytically from the dispersion equation, using the rules of differentiation of implicit functions. In fact, the differentiation of the dispersion equation  $F(v_p, \sigma) = 0$  with respect to  $v_p$  and  $\sigma$  leads to the following differential relation  $(dv_p/d\sigma) \partial F / \partial v_p + (d\sigma/d\sigma) \partial F / \partial \sigma = 0$ . Consequently, the derivative  $dv_p/d\sigma$  can be written as:

$$\frac{dv_p}{d\sigma} = - \frac{\partial F / \partial \sigma}{\partial F / \partial v_p} \tag{17}$$

By virtue of Eqs. 16 and 17 the coefficient of mass sensitivity  $S_\sigma^{v_p}$  is given by the following explicit formula:

where:  $h_1$  is the thickness of the guiding surface layer,  $q_1$  and  $b$  are respectively transverse wavenumbers of the Love wave in the guiding surface layer and in the substrate and  $\partial q_1 / \partial k = - \frac{k}{\sqrt{k_1^2 - k^2}}$ ;  $\partial b / \partial k = \frac{k}{\sqrt{k^2 - k_2^2}}$ .

It has to be stressed that Eq. (18) is a closed form analytical formula for the mass coefficient of sensitivity  $S_{\sigma}^{v_p}$ , as a function of  $\omega, h_1, v_p, c_{44}^{(1)}, c_{44}^{(2)}, \rho_2$ , and  $\sigma$ . Eq. (18) will be used in the subsequent numerical calculations for Love surface waves propagating in waveguides composed of a PMMA guiding surface layer deposited on the ST-Quartz substrate (see Section 8).

**6. Analytical formulas for phase velocity gradients  $-dv_p/dh_1$  and  $-dv_p/df$  of the dispersion curves  $v_p(h_1)$  and  $v_p(f)$**

In this section we will try to find possible correlations between the maximum of the coefficient of sensitivity  $S_{\sigma}^{v_p}$  and the maximum of phase velocity gradients  $-dv_p(h_1)/dh_1$  and  $-dv_p(f)/df$ .

To this end, the author developed in this Section the equations for the phase velocity gradients  $-dv_p(h_1)/dh_1$  and  $-dv_p(f)/df$  in a closed analytical form that can be readily used for numerical calculations.

If the phase velocity  $v_p$  of the Love wave and thickness of the guiding surface layer  $h_1$  are considered as independent variables, the dispersion Eq. 14 can be written in the following implicit form as  $F(v_p, h_1) = 0$ . Using the rules of differentiation of implicit functions from the dispersion relation Eq.14 we obtain:

$$\frac{dv_p}{dh_1} = - \frac{\partial F / \partial h_1}{\partial F / \partial v_p} \tag{19}$$

Consequently, Eq. 19 leads to the following closed-form formula:

$$\left(\frac{dv_p}{dh_1}\right) = \frac{\frac{q_1^2 \cdot (v_p)^3}{\omega^2 \cdot \cos^2(q_1 h_1)} \cdot \left\{ \left(c_{44}^{(1)} q_1\right)^2 + (\sigma \omega^2) \cdot \left(c_{44}^{(2)} b\right) \right\}}{\frac{h_1}{\cos^2(q_1 h_1)} \left\{ \left(c_{44}^{(1)} q_1\right)^2 + (\sigma \omega^2) \cdot \left(c_{44}^{(2)} b\right) \right\} + \tan(q_1 h_1) \left\{ 2q_1 \left(c_{44}^{(1)}\right)^2 - (\sigma \omega^2) \cdot c_{44}^{(2)} \cdot q_1 / b \right\} + c_{44}^{(1)} \cdot \left\{ (\sigma \omega^2) - \left(c_{44}^{(2)} b\right) + c_{44}^{(2)} \cdot q_1^2 / b \right\}} \tag{20}$$

Eq. 20 relates the gradient (slope)  $(dv_p/dh_1)$  of the dispersion curve  $v_p(h_1)$  with material parameters of the Love wave waveguide and frequency  $\omega = 2\pi f$ .

On the other hand, the dispersion Eq. 14 is also an implicit function of  $v_p$  and  $f$ , namely  $F(v_p, f) = 0$ . Therefore, the phase velocity gradient  $(dv_p/df)$  can be expressed as

$$\frac{dv_p}{df} = - \frac{\partial F / \partial f}{\partial F / \partial v_p} \tag{21}$$

Consequently, Eq. 21 leads to the following closed-form analytical formula for the phase velocity gradient  $(dv_p/df)$ :

$$\left(\frac{dv_p}{df}\right) = \frac{\frac{2\pi \cdot q_1 \cdot (v_p)^3}{\omega^3} \left\{ \frac{q_1 h_1}{\cos^2(q_1 h_1)} \left[ \left(c_{44}^{(1)} q_1\right)^2 + (\sigma \omega^2) \cdot \left(c_{44}^{(2)} b\right) \right] + \tan(q_1 h_1) \left\{ 2q_1^2 \left(c_{44}^{(1)}\right)^2 + 3(\sigma \omega^2) \cdot c_{44}^{(2)} \cdot \frac{h_1}{q_1} \right\} + c_{44}^{(1)} q_1 \left\{ (\sigma \omega^2) - 2\left(c_{44}^{(2)} b\right) + 2\sigma \omega^2 \right\} \right\}}{\frac{h_1}{\cos^2(q_1 h_1)} \left\{ \left(c_{44}^{(1)} q_1\right)^2 + (\sigma \omega^2) \cdot \left(c_{44}^{(2)} b\right) \right\} + \tan(q_1 h_1) \left\{ 2q_1 \left(c_{44}^{(1)}\right)^2 - (\sigma \omega^2) \cdot c_{44}^{(2)} \cdot q_1 / b \right\} + \left(c_{44}^{(1)}\right) \cdot \left\{ (\sigma \omega^2) - \left(c_{44}^{(2)} b\right) \left(1 - q_1^2 / b^2\right) \right\}} \tag{22}$$

Similarly to formula 20, Eq. 22 relates the gradient (slope)  $(dv_p/f)$  of

the dispersion curve  $v_p(f)$  with material parameters of the Love wave waveguide, wave frequency  $\omega$  and thickness of the guiding surface layer  $h_1$ , etc.

At first glance, Eq. 20, 22 and 18, may look somewhat intimidating but in fact they are quite elementary and easy to implement in numerical calculations (see Section 8).

Having developed the analytical formulas for  $S_{\sigma}^{v_p}$  and  $dv_p/df$ ,  $dv_p/dh_1$  in the next Section 7 we will seek for possible relations between them. Our attention will be focused on points where the relative gradients  $-(1/v_p)dv_p/dh_1$ ,  $-(1/v_p)dv_p/df$  of the dispersion curves, and the mass sensitivity  $S_{\sigma}^{v_p}$  attain maxima.

**7. Relation between phase velocity gradients  $-dv_p/dh_1$ ,  $-dv_p/df$  and the mass sensitivity  $S_{\sigma}^{v_p}$**

The mathematical analysis of the dispersion Eq. 14 allows to develop the analytical equations relating the mass sensitivity  $S_{\sigma}^{v_p}$  with the phase velocity gradients  $dv_p/dh_1$ ,  $-dv_p/df$ .

Employing Eqs. 17 and 19 it can be shown that the mass sensitivity  $S_{\sigma}^{v_p}$  and phase velocity gradient  $-dv_p/dh_1$  are related by the following differential formula:

$$S_{\sigma}^{v_p} = \frac{\partial F / \partial \sigma}{\partial F / \partial h_1} \cdot \frac{1}{v_p} \cdot \left(\frac{dv_p}{dh_1}\right) \tag{23}$$

Thus, differentiation of the dispersion equation  $F(\sigma, h_1) = 0$  (Eq. 14) with respect to  $\sigma$  and  $h_1$  and employment of Eq. 23 lead to:

$$S_{\sigma}^{v_p} = \frac{\omega^2 \cdot \cos^2(q_1 h_1)}{q_1} \cdot \frac{\left\{ \tan(q_1 h_1) \cdot \left(c_{44}^{(2)} b\right) + \left(c_{44}^{(1)} q_1\right) \right\}}{\left\{ \left(c_{44}^{(1)} q_1\right)^2 + (\sigma \omega^2) \cdot \left(c_{44}^{(2)} b\right) \right\}} \cdot \frac{1}{v_p} \cdot \left(\frac{dv_p}{dh_1}\right) \tag{24}$$

Eq. 24 is an analytical formula that relates the mass sensitivity  $S_{\sigma}^{v_p}$  with the relative gradient  $-(1/v_p)dv_p/dh_1$  of the dispersion curve  $v_p(h_1)$  of the Love wave, propagating in the waveguide structure shown in Fig. 1.

It should be stressed that Eq. 24 was developed without any simplifying assumptions from the dispersion Eq. 14, obtained from the

full wave theory presented in Section 3.

Eq. 24 shows that the mass sensitivity  $S_{\sigma}^{v_p}$  depends critically on the operation point on the dispersion curve  $v_p(h_1)$ . In fact, Eq. 24

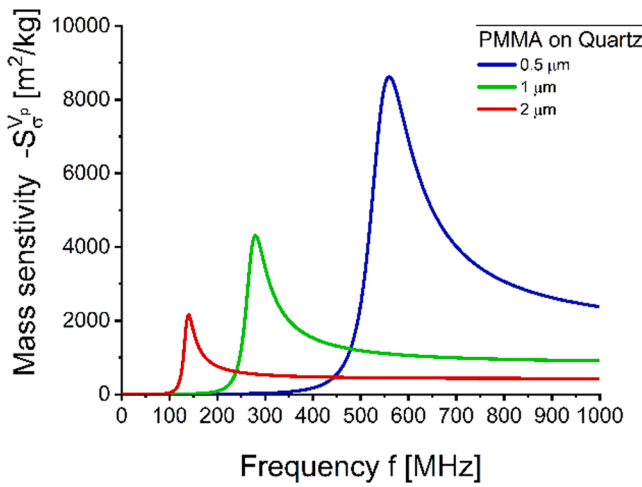


Fig. 2. Mass sensitivity  $S_{\sigma}^{V_p}$  [ $m^2/kg$ ] for Love surface waves propagating in the PMMA- Quartz waveguide shown in Fig. 1, as a function of wave frequency  $f$ , for different values of thickness  $h_1$  of the guiding PMMA surface layer ( $h_1 = 0.5, 1$  and  $2 \mu m$ ).

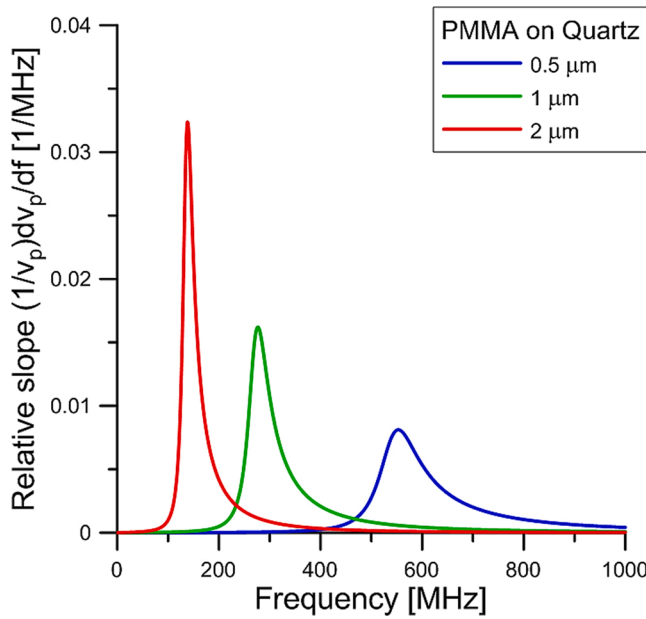


Fig. 3. Relative phase velocity gradient  $-(1/v_p)dv_p/df$  of the dispersion curve  $v_p(f)$ , as a function of frequency  $f$ , for Love waves propagating in the PMMA-Quartz waveguide shown in Fig. 1.

demonstrates that the mass coefficient of sensitivity  $S_{\sigma}^{V_p}$  is actually proportional to the relative phase velocity gradient  $-(1/v_p)dv_p/dh_1$ . As a result, the maximum of the mass sensitivity  $S_{\sigma}^{V_p}$  and the maximum of the relative gradient  $-(1/v_p)dv_p/dh_1$ , will occur virtually for the same value of thickness  $h_1$  of the guiding surface layer. This is a very important conclusion enabling for optimum design of Love wave devices with high sensitivities.

Similarly, employing Eqs. 17 and 21 and the dispersion equation  $F(\sigma, f) = 0$  (Eq.14), it is straightforward to show that the mass coefficient of sensitivity  $S_{\sigma}^{V_p}$  can be expressed by the following differential formula:

$$S_{\sigma}^{V_p} = \frac{\partial F / \partial \sigma}{\partial F / \partial f} \cdot \frac{1}{v_p} \left( \frac{dv_p}{df} \right) \quad (25)$$

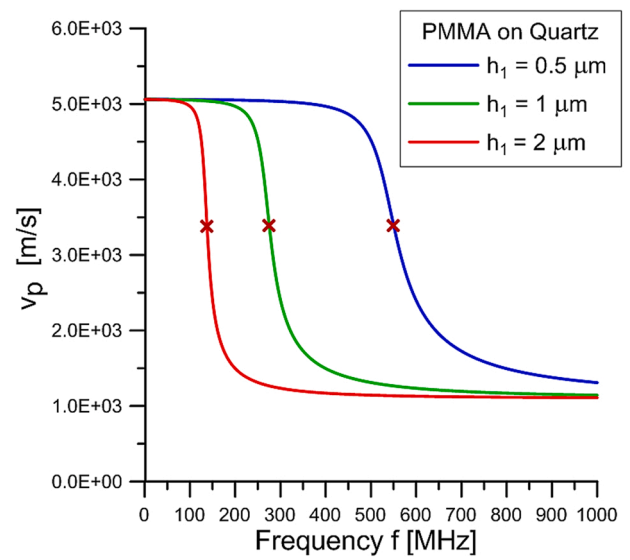


Fig. 4. Phase velocity dispersion curves  $v_p(f)$  of the Love wave propagating in the PMMA-Quartz waveguide structure shown in Fig. 1. The maxima of the relative slope  $-(1/v_p)dv_p/df$ , are marked with the cross "x".

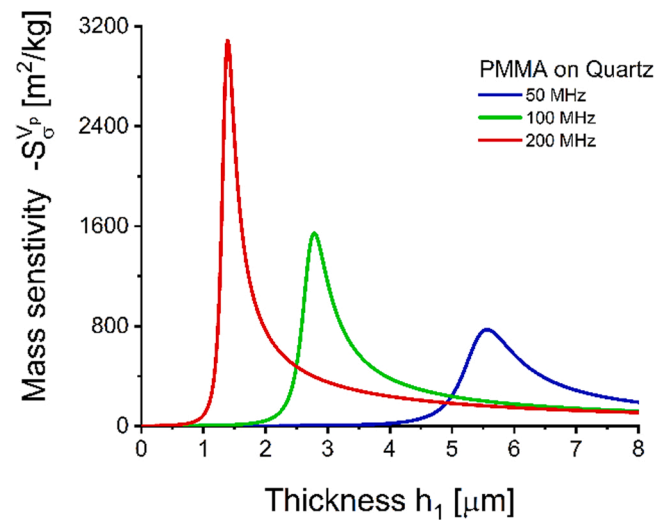


Fig. 5. Mass sensitivity  $S_{\sigma}^{V_p}$  [ $m^2/kg$ ] for Love surface waves propagating in PMMA-Quartz waveguides, shown in Fig. 1, as a function of thickness  $h_1$  of the PMMA guiding surface layer, for different values of wave frequency  $f = 50, 100$  and  $200 MHz$ .

Table 2

Maximum values of the relative phase velocity gradient  $-(1/v_p)dv_p/df$ , mass sensitivity  $S_{\sigma}^{V_p}$ , and the corresponding frequencies  $f_{max}$  of the maxima for Love waves propagating in PMMA-Quartz waveguides. Thickness of the guiding PMMA surface layer  $h_1 = 0.5, 1$  and  $2 \mu m$ .

$h_1$ $\mu m$	$-(1/v_p)dv_p/df$ (Fig 3), (Eq.22)		$S_{\sigma}^{V_p}$ (Fig 2), (Eq.18)	
	$f_{max}$ MHz	max 1/MHz	$f_{max}$ MHz	max $m^2/kg$
0.5	552	0.8106e-2	559	8623
1.0	277	0.1596e-1	280	4310
2.0	138	0.3236e-1	140	2155

Differentiating the dispersion equation  $F(\sigma, f) = 0$  with respect to the surface mass density  $\sigma$  and wave frequency  $f$  from Eq.25 one obtains:

$$S_{\sigma}^{v_p} = \frac{\omega^3}{2\pi} \cdot \frac{\tan(q_1 h_1) \bullet (c_{44}^{(2)} b) + c_{44}^{(1)} q_1}{\frac{q_1 h_1}{\cos^2(q_1 h_1)} \left[ (c_{44}^{(1)} q_1)^2 + \sigma \omega^2 c_{44}^{(2)} b \right] + \tan(q_1 h_1) \bullet \sigma \omega^2 c_{44}^{(2)} b + \sigma \omega^2 c_{44}^{(1)} q_1} \bullet \frac{1}{v_p} \bullet \left( \frac{dv_p}{df} \right) \quad (26)$$

Eq. 26 shows that the mass sensitivity  $S_{\sigma}^{v_p}$  is in fact also proportional to the relative phase velocity gradient  $-(1/v_p)dv_p/df$ . As a result, the maximum of the mass sensitivity  $S_{\sigma}^{v_p}$  and the maximum of the relative gradient  $-(1/v_p)dv_p/df$  will occur virtually at the same frequency  $f$ . This is a very important conclusion allowing for optimum design of Love wave devices with high sensitivities.

### 8. Results of numerical calculations

The dispersion curves  $v_p(h_1)$ ,  $v_p(f)$ , their gradients  $dv_p/dh_1$ ,  $dv_p/df$  and mass coefficient of sensitivity  $S_{\sigma}^{v_p}$  were evaluated numerically using formulas no 14, 18, 20 and 22 developed in Sections 3, 4, 5 and 6. The propagation of Love surface waves was evaluated in the exemplary waveguide structure composed of the PMMA surface layer deposited on ST-Quartz substrate, with the parameters given in Table 1.

In the numerical calculations, we selected the following initial surface mass density:  $\sigma = 1 \times 10^{-6}$  [kg/m<sup>2</sup>].

The mass sensitivity  $S_{\sigma}^{v_p}$  was plotted as a function of wave frequency  $f$  (Fig. 2) and thickness  $h_1$  of the PMMA guiding surface layer (Fig. 5).

From Fig. 2 it is apparent that the mass coefficient of sensitivity  $S_{\sigma}^{v_p}$  starts from zero for low frequencies  $f$ , displays subsequently resonant like peaks, and gradually decreases to zero for higher frequencies, when  $f \rightarrow +\infty$ .

Using formula 22, we plot in Fig. 3 the relative phase velocity gradient  $-(1/v_p)dv_p/df$  as a function of frequency  $f$ , for Love waves propagating in the analyzed PMMA-Quartz waveguide structure, shown in Fig.1.

Similarly to the mass sensitivity  $S_{\sigma}^{v_p}$  shown in Fig. 2, the relative gradient  $-(1/v_p)dv_p/df$  of the dispersion curve  $v_p(f)$  plotted in Fig. 3, displays also resonant-like maxima, as a function of frequency  $f$ .

The numerical results calculated for maxima of the relative phase velocity gradient  $-(1/v_p)dv_p/df$ , and the mass coefficient of sensitivity  $S_{\sigma}^{v_p}$ , plotted in Fig. 2 and 3, are summarized in Table 2.

Phase velocity dispersion curves  $v_p(f)$  of the Love wave propagating in the PMMA-Quartz waveguide are shown in Fig.4. From Fig. 4 it is clear that the maxima of the relative slope  $-(1/v_p)dv_p/df$ , (marked by the cross) occur approximately halfway down the slope of the dispersion curve  $v_p(f)$ .

Using the formula Eq.18 we also plotted in Fig. 5 the mass sensitivity  $S_{\sigma}^{v_p}$  of the Love wave sensor, as a function of the thickness  $h_1$  of the guiding surface layer.

From Fig. 5 it is evident that the mass coefficient of sensitivity  $S_{\sigma}^{v_p}$  starts from zero for low values of  $h_1$ , shows subsequently resonant like peaks and gradually drops to zero for larger values of the surface layer thickness  $h_1$ .

The plot of the relative gradient  $-(1/v_p)dv_p/dh_1$  of the Love wave dispersion curve  $v_p(h_1)$ , as a function of the thickness  $h_1$  of the surface layer, is given in Fig.6.

The plots of the relative gradient  $-(1/v_p)dv_p/dh_1$  of the Love wave dispersion curve  $v_p(h_1)$ , see Fig.6, also displays resonant-like maxima as a function of the surface layer thickness  $h_1$ .

To visualize the location of the points with the maximum gradient of the dispersion curve  $v_p(h_1)$ , the dispersion curves  $v_p(h_1)$ , as a function of the surface layer thickness  $h_1$  were plotted in Fig. 7. The maxima of the relative gradient  $-(1/v_p)dv_p/dh_1$  are marked with the cross.

The results for the maximum of the relative gradient  $-(1/v_p)dv_p/dh_1(h_1)$  and the mass coefficient of sensitivity  $S_{\sigma}^{v_p}$ , plotted in

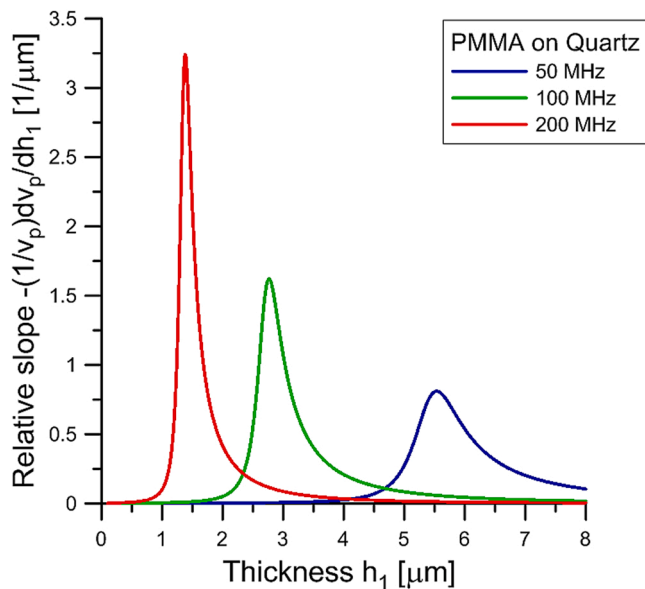


Fig. 6. Relative gradient  $-(1/v_p)dv_p/dh_1$  of the dispersion curve  $v_p(h_1)$  as a function of thickness  $h_1$  of the guiding PMMA surface layer of the Love wave propagating in the PMMA-Quartz waveguide shown in Fig. 1.

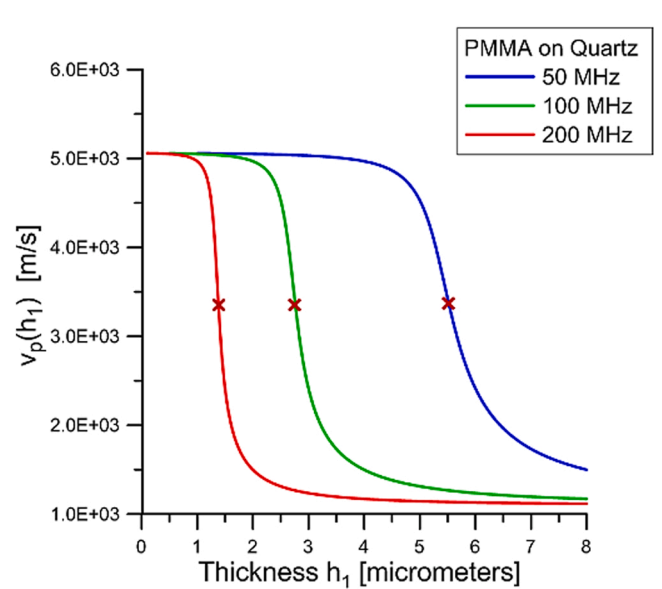


Fig. 7. Phase velocity dispersion curves  $v_p(h_1)$  of the Love wave propagating in the PMMA-Quartz waveguide shown in Fig. 1. The maxima of the relative slope  $-(1/v_p)dv_p/dh_1(h_1)$  are marked with the cross.

**Table 3**

Maximum values of the relative phase velocity gradient (slope)  $-(1/v_p)dv_p/dh_1$ , mass sensitivity  $S_\sigma^y$ , and the corresponding thickness  $h_{1max}$  of the maxima, for Love waves propagating in the PMMA-Quartz waveguide shown in Fig.1. Wave frequency  $f = 50, 100$  and  $200$  MHz.

$f$ MHz	$-(1/v_p)dv_p/dh_1$ (Fig.6), (Eq.20)		$-S_\sigma^y$ (Fig.5), (Eq.18)	
	$h_{1max}$ $\mu\text{m}$	max $1/\mu\text{m}$	$h_{1max}$ $\mu\text{m}$	max $\text{m}^2/\text{kg}$
50	5.536	0.8095	5.565	772.5
100	2.767	1.6194	2.782	1545
200	1.383	3.2400	1.391	3092

Figs. 5 and 6 are summarized in Table 3.

## 9. Discussion

The mass coefficient of sensitivity  $S_\sigma^y$  is a very important parameter of Love wave waveguides that quantifies the quality of Love wave devices. The coefficient of mass sensitivity  $S_\sigma^y$  relates the change in the phase velocity  $v_p$  of the Love wave with the surface density  $\sigma$  of an infinitesimally thin layer of mass, deposited on top of the guiding surface layer of the waveguide.

In general, the dispersion equation (Eq.14) of the Love surface wave can be regarded as an implicit function of the phase velocity  $v_p$ , surface mass density  $\sigma$  loading free surface of the waveguide, thickness  $h_1$  of the surface layer and wave frequency  $f$ . The dispersion equation (Eq.14) can be expressed symbolically as  $F_2(v_p, \sigma, h_1, f) = 0$ .

Applying the theorem of differentiation of implicit functions, the author has developed in this paper novel analytical formulas for the mass coefficient of sensitivity  $S_\sigma^y$ , and phase velocity gradients  $dv_p/dh_1$ ,  $dv_p/df$ , as a function of thickness  $h_1$  of the guiding surface layer and wave frequency  $f$ .

The developed analytical formulas for  $S_\sigma^y$ ,  $-(1/v_p)dv_p/dh_1$  and  $-(1/v_p)dv_p/df$  depend explicitly on: 1) material parameters of the waveguide, 2) surface layer thickness  $h_1$ , and 3) wave frequency  $f$ , as well as 4) surface mass density  $\sigma$  loading top surface of the waveguide.

In Section 7 the author discovered new relations between the mass coefficient of sensitivity  $S_\sigma^y$  and the relative phase velocity gradients  $-(1/v_p)dv_p/dh_1$  and  $-(1/v_p)dv_p/df$ , see Eqs. 24 and 26, showing that  $S_\sigma^y$  is in fact proportional to  $-(1/v_p)dv_p/dh_1$  and  $-(1/v_p)dv_p/df$ . Consequently, the maximum of the coefficient of mass sensitivity  $S_\sigma^y$  and the maximum of relative phase velocity gradients occur virtually at the same thickness  $h_1$  of the guiding surface layer and wave frequency  $f$ . This property is of crucial practical importance in design of Love wave devices (e.g., sensors) since the maximum of the mass sensitivity occurs at the point of the steepest descent of the dispersion curves as a function of frequency  $f$  or thickness of the surface layer  $h_1$  of the waveguide.

The analytical model, developed by the author, for mass sensitivity of Love wave waveguides (Eqs. 18, 20, 22, 24 and 26) can provide a very useful tool for optimum design of Love wave devices with enhanced mass sensitivities.

## 10. Conclusions

From the analytical and numerical results obtained in this paper we can draw the following conclusions:

1. The analytical formulas (Eqs. 18, 20 and 22) for: 1) mass sensitivity  $S_\sigma^y$ , 2) gradient  $dv_p/dh_1$  of the dispersion curve  $v_p(h_1)$  and 3) gradient  $dv_p/df$  of the dispersion curve  $v_p(f)$ , developed by the author are new and were not yet published in the literature.
2. Similarly, the analytical formulas (Eqs.24 and 26) that relate the mass sensitivity  $S_\sigma^y$  of the Love wave sensors with the relative slopes  $-(1/v_p)dv_p/dh_1$  and  $-(1/v_p)dv_p/df$  of the dispersion curves  $v_p(h_1)$

and  $v_p(f)$ , were developed by the author for the first time and were not yet published in the literature.

3. The mass sensitivity of the Love wave  $S_\sigma^y$  exhibits pronounced maxima as a function of both: a) the thickness  $h_1$  of the surface layer and b) wave frequency  $f$ , see Figs. 2 and 5.
4. Analogous maxima can also be found in the relative slopes of the phase velocity  $v_p$  dispersion curve as a function of thickness  $h_1$  of the surface layer:  $-(1/v_p)dv_p/dh_1$  and wave frequency  $f$ :  $-(1/v_p)dv_p/df$ , see Figs. 3 and 6.
5. The maxima of the mass sensitivity  $S_\sigma^y$  and the relative gradients  $-(1/v_p)dv_p/dh_1$ ,  $-(1/v_p)dv_p/df$ , occur virtually at the same points of the thickness  $h_1$  and frequency  $f$ , see Tables 2 and 3.
6. The analytical formulas (Eqs. 24 and 26) developed by the author for the first time show that the mass sensitivity  $S_\sigma^y$  and the relative slopes  $-(1/v_p)dv_p/dh_1$ ,  $-(1/v_p)dv_p/df$  are in fact proportional to each other.
7. Employment of the analytical formulas developed by the author for the mass sensitivity  $S_\sigma^y$  (Eq.18) and phase velocity gradients  $dv_p(f)/df$ ,  $dv_p(h_1)/dh_1$  (Eq. 20, 22) can significantly improve the design process of Love wave devices.

By contrast to pure numerical methods, such as (FEM), the closed-form analytical formulas developed for the first time in this paper have many advantages such as very high speed of execution in numerical implementations and even more importantly the possibility for a direct parametric optimization of the Love wave waveguide as a function of its material parameters, thickness of the guiding surface layer  $h_1$  and wave frequency  $f$ .

The results of this study can be very useful for engineers and scientists working in the design, modeling and optimization of ultrasonic Love wave devices.

## CRedit authorship contribution statement

**Piotr Kielczyński:** Conceptualization, Methodology, Software, Writing – original draft preparation, Writing – review & editing.

## Declaration of Competing Interest

The authors declare that they have no known competing financial interests or personal relationships that could have appeared to influence the work reported in this paper.

## Acknowledgment

The project was funded by the National Science Centre (Poland), granted on the basis of Decision No. 2016/21/B/ST8/02437.

## References

- [1] D.S. Ballantine, R.M. White, S.J. Martin, A.J. Ricco, E.T. Zellers, G.C. Frye, H. Wohltjen, Acoustic Wave Sensors. Theory, Design, and Physico-Chemical Applications, Academic Press, San Diego, 1997.
- [2] M.I. Rocha Gaso, Y. Jiménez, L.A. Francs, A. Arnau, Love wave biosensors: a review, in: T. Rincken (Ed.), State of the Art in Biosensors, IntechOpen, Rijeka, 2013, pp. 277–310, <https://doi.org/10.5772/53077>.
- [3] A. Vikström, M.V. Voinova, Soft-film dynamics of SH-SAW sensors in viscous and viscoelastic fluids, Sens. Bio-Sens. Res. (2016) 78–85, <https://doi.org/10.1016/j.sbsr.2016.08.004>.
- [4] X. Chen, D. Liu, Analysis of viscosity sensitivity for liquid property detection applications based on SAW sensors, Mater. Sci. Eng. C 30 (2010) 1175–1182, <https://doi.org/10.1016/j.msec.2010.06.008>.
- [5] P. Kielczyński, M. Szalewski, An inverse method for determining the elastic properties of thin layers using Love surface waves, Inverse Probl. Sci. Eng. 19 (2011) 31–43, <https://doi.org/10.1080/17415977.2010.531472>.
- [6] P. Kielczyński, M. Szalewski, A. Balcerzak, Inverse procedure for simultaneous evaluation of viscosity and density of Newtonian liquids from dispersion curves of Love waves, J. Appl. Phys. 116 (7) (2014), 044902, <https://doi.org/10.1063/1.4891018>.

- [7] P. Kielczyński, M. Szalewski, A. Balcerzak, K. Wieja, Group and phase velocity of Love waves propagating in elastic functionally graded materials, *Arch. Acoust.* 40 (2015) 273–281, <https://doi.org/10.1515/aoa-2015-0030>.
- [8] P. Kielczyński, M. Szalewski, A. Balcerzak, K. Wieja, Propagation of ultrasonic Love wave in non-homogeneous elastic functionally graded materials, *Ultrasonics* 65 (2016) 220–227, <https://doi.org/10.1016/j.ultras.2015.10.001>.
- [9] P. Kielczyński, M. Szalewski, A. Balcerzak, K. Wieja, Dispersion curves of Love waves in elastic waveguides loaded with a Newtonian liquid layer of finite thickness, *Arch. Acoust.* 40 (2020) 19–27, <https://doi.org/10.24425/aoa.2019.129738>.
- [10] H. Wu, X. Xiong, H. Zu, J.H.-C. Wang, Q.-M. Wang, Theoretical analysis of a Love wave biosensor in liquid with a viscoelastic wave guiding layer, *J. Appl. Phys.* 121 (2017) 054501–054542, <https://doi.org/10.1063/1.4975112>.
- [11] P. Kielczyński, Direct Sturm–Liouville problem for surface Love waves propagating in layered viscoelastic waveguides, *Appl. Math. Model.* 53 (2018) 419–432, <https://doi.org/10.1016/j.apm.2017.09.013>.
- [12] K. Takayanagi, J. Kondoh, Improvement of estimation method for physical properties of liquid using shear horizontal surface acoustic wave sensor response, *Jpn. J. Appl. Phys.* 57 (2018) 07LD02, <https://doi.org/10.7567/JJAP.57.07LD02>.
- [13] A. El Baroudi, J.Y. Le Pommellec, Viscoelastic fluid effect on the surface wave propagation, *Sens. Actuators A* 291 (2019) 188–195, <https://doi.org/10.1016/j.sna.2019.03.039>.
- [14] A. Abdollahi, Z. Jiang, S.A. Arabshani, Evaluation on mass sensitivity of SAW sensors for different piezoelectric materials using Finite-Element analysis, *IEEE Trans. Ultrason. Ferroelectr. Freq. Control* 54 (2007) 2446–2455, <https://doi.org/10.1109/TUFFC.2007.558>.
- [15] M.I. Rocha-Gaso, R. Fernandez-Diaz, A. Arnau-Vives, Mass sensitivity evaluation of a Love wave sensor using the 3D Finite Element Method, *IEEE Ultrasonic Symposium Proceedings*, (2010) 228–231, San Diego, USA.
- [16] G. McHale, M.I. Newton, F. Martin, Theoretical mass sensitivity of Love wave and layer guided acoustic plate mode sensors, *J. Appl. Phys.* 91 (2002) 9701–9710.
- [17] G. McHale, M.I. Newton, F. Martin, Theoretical mass, liquid, and polymer sensitivity of acoustic wave sensors with viscoelastic guiding layers, *J. Appl. Phys.* 93 (2003) 675–690.
- [18] K.M. Mohibul Kabir, Glenn I. Matthews, Ylias M. Sabri, Salvy P. Russo, Samuel J. Ippolito, Suresh K. Bhargava, Development and experimental verification of a finite element method for accurate analysis of a surface acoustic wave device, *Smart Mater. Struct.* 25 (2016), 035040.
- [19] T. Wang, R. Green, R. Guldiken, J. Wang, S. Mohapatra, S.S. Mohapatra, Finite element analysis for surface acoustic wave device characteristic properties and sensitivity, *Sensors* 19 (2019) 1749, <https://doi.org/10.3390/s19081749>.
- [20] T. Wang, R. Murphy, J. Wang, S.S. Mohapatra, S. Mohapatra, R. Guldiken, Perturbation analysis of a multiple layer guided love wave sensor in a viscoelastic environment, *Sensors* 19 (2019) 4533, <https://doi.org/10.3390/s19204533>.
- [21] A. Rasmusson, E. Gizeli, Comparison of Poly(methylmethacrylate) and Novolak waveguide coatings for an acoustic biosensor, *J. Appl. Phys.* 90 (2001) 5911–5914, <https://doi.org/10.1063/1.1405142>.
- [22] J. Kushibiki, I. Takanaga, S. Nishiyama, Measurements of the acoustical physical constants of synthetic-quartz for SAW devices, *IEEE Trans. Ultrason. Ferroelectr. Freq. Control* 49 (2002) 125–135, <https://doi.org/10.1109/58.981390>.
- [23] S.-Y. Chu, W. Water, J.-T. Liaw, An investigation of the dependence of ZnO film on the sensitivity of Love mode sensor in ZnO/quartz structure, *Ultrasonics* 41 (2003) 133–139, [https://doi.org/10.1016/S0041-624X\(02\)00430-4](https://doi.org/10.1016/S0041-624X(02)00430-4).
- [24] Z. Xu, Y.J. Yuan, Implementation of guiding layers of surface acoustic wave devices: a review, *Biosens. Bioelectron.* 99 (2018) 500–512, <https://doi.org/10.1016/j.bios.2017.07.060>.
- [25] J.D. Achenbach, *Wave Propagation in Elastic Solids*. Amsterdam: North-Holland (1973).
- [26] J.L. Rose, *Ultrasonic Guided Waves in Solid Media*, Cambridge University Press, Cambridge, 2014.
- [27] B.A. Auld, *Acoustic Fields and Waves in Solids*, Krieger Publishing Company, Florida, 1990.
- [28] W.T. Thomson, Transmission of elastic waves through a stratified solid medium, *J. Appl. Phys.* 21 (1950) 89–93.
- [29] N.A. Haskell, The dispersion of surface waves on multilayered media, *Bull. Seismol. Soc. Am.* 43 (1953) 17–34.
- [30] G.H. Ke, H. Dong, M. Kristensen, Thompson M. Modified Thomson Haskell matrix methods for surface-wave dispersion-curve calculation and their accelerated root-searching schemes, *Bull. Seismol. Soc. Am.* 101 (2011) 1692–1703, <https://doi.org/10.1785/0120100187>.